



Research article

Exploring the environmental contamination toxicity and potential carcinogenic pathways of perfluorinated and polyfluoroalkyl substances (PFAS): An integrated network toxicology and molecular docking strategy

Zhi Lin, Yvmo Li, Jiarui Zhao, Jun Li, Shuang Pan, Xinhe Wang, He Lin^{*},
Zhe Lin^{**}

College of Pharmacy, Changchun University of Chinese Medicine, China

ARTICLE INFO

Keywords:

Network toxicology
Molecular docking
PFAS
Carcinogenic pathways

ABSTRACT

The objective of this study was to investigate the potential carcinogenic toxicity and mechanisms of PFAS in thyroid, renal, and testicular cancers base on network toxicology and molecular docking techniques. Structural modeling was performed to predict relevant toxicity information, and compounds and cancer-related targets were screened in multiple databases. The interaction of PFAS with three cancers and their key protein targets were explored by combining protein network analysis, enrichment analysis and molecular docking techniques. PFOA, PFOS, and PFHXS exhibited significant carcinogenic and cytotoxic effects. These compounds may induce cancer by mediating active oxygen metabolism and the transduction of phosphatidylinositol 3-kinase/protein kinase B signaling pathway through genes such as ALB, mTOR, MDM2, and ERBB2. Furthermore, the underlying toxic mechanisms may be linked to the pathways in cancer, chemical carcinogenesis through reactive oxygen species/receptor activation, and the FoxO signaling pathway. The results contribute to a comprehensive understanding of the effects of these environmental pollutants on genes, proteins, and metabolic pathways in living organisms. It revealed their toxicity mechanisms in inducing thyroid, renal, and testicular cancers, and provided a solid theoretical foundation for designing new environmental control strategies and drug screening initiatives. Additionally, the integrated application of network toxicology and molecular docking technology can enhance our understanding of the toxicity and mechanisms of unknown environmental pollutants, which is beneficial for protecting the environment and human health.

1. Introduction

Per- and polyfluoroalkyl substances (PFAS) are synthetic, multifunctional chemicals characterized by a hydrophilic head and a hydrophobic, fluorine-saturated carbon chain, i.e., the C-F bond [1,2]. This molecular structure renders PFAS extremely chemically

^{*} Corresponding author. College of Pharmacy, Changchun University of Chinese Medicine, NO. 1035 Boshuo Road, Changchun, Jilin, 130117, China.

^{**} Corresponding author. College of Pharmacy, Changchun University of Chinese Medicine, NO. 1035 Boshuo Road, Changchun, Jilin, 130117, China.

E-mail addresses: linhe@ccucm.edu.cn (H. Lin), linzhe1228@163.com (Z. Lin).

<https://doi.org/10.1016/j.heliyon.2024.e37003>

Received 9 August 2024; Accepted 26 August 2024

Available online 28 August 2024

2405-8440/© 2024 The Authors. Published by Elsevier Ltd. This is an open access article under the CC BY-NC-ND license (<http://creativecommons.org/licenses/by-nc-nd/4.0/>).

and thermally stable, making them widely used in industrial and agricultural production [3], as well as in everyday consumer products such as clothing, furniture, food packaging, and electrical appliances [4–6]. Therefore, it is unsurprising that humans are routinely exposed to PFAS throughout their lives. However, due to the large volume of industrial emissions, the stable nature of PFAS makes them difficult to degrade once released into the environment [7]. Owing to their water solubility, mobility, persistence, and bioaccumulation, PFAS are prone to migrate and accumulate in various environmental matrices and living organisms [8–10], and have even been labeled as “permanent chemicals” [11]. There are more than 4700 known PFAS chemicals and this number continues to grow as new chemicals are invented in industry [12]. Three of these compounds, PFOA (perfluorooctanoic acid), PFOS (perfluorooctane sulfonate) and PFHXS (perfluorohexane sulfonate), have been produced for the longest period of time, are the most widely distributed in the environment, and may adversely affect terrestrial and aquatic ecosystems or pose risks to human health. A study assessing water quality in the Oder River, Poland, identified 14 PFAS compounds, with more than half of the water samples exceeding the ambient PFOS quality standard of 0.65 ng/L [13]. PFAS can accumulate in drinking water and food through migration [14,15], so sources such as drinking water, food (including contamination from food packaging), and indoor dust are considered major pathways for human exposure to PFAS [16].

From epidemiological data, PFAS have been identified as hepatotoxic, immunotoxic, neurotoxic, and reproductively toxic, and are now found extensively in human body fluids, including the placenta [17,18]. Perfluorooctanoic acid (PFOA) and perfluorooctane sulfonate (PFOS) are the most predominant and commonly detected PFAS in human blood [19]. Long-term exposure to PFAS in humans has been associated with abnormal liver function [20], dyslipidemia [21], cardiovascular disease [22], adverse effects on fetal growth, and an array of cancers. Some studies have shown that PFAS pose a risk of causing thyroid cancer [23]. Other studies have found PFAS in human semen. Notably, compounds such as PFOA and PFOS are inversely associated with human semen parameters, including sperm count, morphology, and motility, highlighting a potential threat to male fertility [24]. Among PFAS, perfluorooctanoic acid (PFOA) and perfluorooctane sulfonic acid (PFOS), along with their derivatives, have been classified as persistent organic pollutants (POPs) under the Stockholm Convention [25]. In 2023, the Chinese Ministry of Ecology and Environment also included PFOA, PFOS and perfluorohexane sulfonate acid (PFHXS) in the list of new pollutants for key control. However, PFAS may induce toxicity through a variety of biomolecular networks, and their potential virulence mechanisms are complex. Therefore, scientific methods to assess the toxicity of PFAS and explore their potential toxicity mechanisms are necessary.

Network toxicology excels by utilizing multiple databases to gather accurate compound information and integrating diverse bioinformatics data. This integration enables the construction of a comprehensive network mapping compounds to disease targets [26]. It can transform the complex multi-target toxicity mechanisms of target compounds into intuitive graphical models, thereby enabling a thorough and systematic exploration of toxicity at the molecular level in organisms. Another significant advantage of network toxicology is its high throughput and efficiency, which enable the rapid screening of potential toxic substances through computational simulations and data mining. It not only reduces experimental costs and time but also enhances the overall efficiency of toxicity assessments. Molecular docking technology can simulate the interaction between target compounds and biomolecules, predicting the affinity and potential biological activities of the two. This technique enables us to precisely identify the interactions between compounds and disease targets at the molecular level and to understand the protein-binding sites involved in their pathogenicity. The integration of network toxicology and molecular docking provides a comprehensive, efficient, and precise methodology for evaluating the toxicity and efficacy of compounds. This collaborative strategy contributes to advances in environmental toxicology, drug discovery and other fields.

In view of the chemical stability and bioaccumulation potential of PFAS, their hazards to the environment and human health have raised significant concerns. Among them, PFOA, PFOS, and PFHXS are especially noteworthy due to their prolonged use and extensive detection. It is, therefore, vital to understand the carcinogenic potential and mechanism of these three compounds for public health. On the other hand, there are more numerous clinical studies on PFOA, PFOS, and PFHXS causing liver cancer and cardiovascular diseases. However, in recent years, these three compounds have been found to have a potential risk for thyroid, kidney, and testicular cancers, among others. The related research in these areas remains unsystematic and relatively scarce. In addition, the three compounds, PFOS, PFOA, and PFHXS, are structurally similar but may differ in their toxicological characteristics and mechanisms of action. Therefore, we selected the three main compounds of PFAS, PFOA, PFOS, and PFHXS, and used network toxicology and molecular docking techniques to investigate the toxic effects and potential toxicity mechanisms of the three compounds on thyroid cancer (hereinafter referred to as ThC), renal cancer (hereinafter referred to as KC), and testicular cancer (hereinafter referred to as TeC), aiming to elucidate the potential toxicity mechanisms of PFAS in the biological organism and fill the gap in the field of toxicity, to provide a theoretical basis for the risk assessment and regulatory control system of PFAS, and to provide a reference for clinical treatment.

2. Methods

The research data was sourced from online database platforms. Details regarding the specific database names and their respective URLs were provided in [Supplementary Table 1](#).

2.1. Network toxicology predictive analysis of PFOA, PFOS, and PFHXS

“Perfluorooctanoic acid (PFOA)”, “perfluorooctanesulfonic acid (PFOS)” and “perfluorooctanesulfonic acid (PFHXS)” were queried as search terms in the PubChem database to determine the standard structure and canonical SMILES codes for PFOA, PFOS and PFHXS. The SMILES encoding of the above three PFAS compounds was entered into three analytical tools, ProTox 3.0, ADMETlab 2.0 and Vnn-ADMET. Through the structural modeling capabilities of these platforms, the toxicity characteristics of PFOS, PFOA and PFHXS were

predicted, thus gaining a preliminary understanding of their toxicological characteristics.

2.2. Targets collection for PFOA, PFOS, PFHXS

The ChEMBL database was used to identify potential targets of PFOA, PFOS and PFHXS with the keywords “perfluorooctanoic acid (PFOA)”, “perfluorooctanoic acid (PFOS)” and “perfluorooctanoic acid (PFHXS)” and the species selection was set as “*Homo sapiens*” [27]. Subsequently, the Canonical SMILES codes of these compounds were uploaded to the STITCH, SwissTarget Prediction, and PharmMapper databases. In the SwissTarget Prediction database, targets with “Probability >0” were filtered [28]. The target data collected from these databases was then consolidated, duplicates were removed, and the target names were standardized using the Uniprot database [29]. This process culminated in the establishment of a comprehensive target database on PFAS.

2.3. Collection of targets related to ThC, KC and TeC

“Thyroid cancer,” “kidney/kidney cancer,” and “testicular cancer” were used as search terms in GeneCards, OMIM, DrugBank, TTD, and DisGeNET databases. OMIM database selected targets with *; the DisGeNET database selected targets with “Score_gda >0.1”; and the GeneCards database selected targets with “Relevance score ≥ 0.5 ” targets. After integrating the disease target information from these databases, the duplicate data was deleted and three distinct disease target databases for PFOA, PFOS and PFHXS, were established respectively.

2.4. Protein-protein interaction (PPI) network construction and core target screening

The intersection analysis was performed using the PFAS target database established in Section 2.2 and the three disease target databases created in Section 2.3. The Venn diagrams were constructed using intersecting targets of PFAS-related ThC, KC, and TeC. These intersecting targets were identified as potential toxicity targets for PFAS induced diseases. In the STRING database, the targets were entered into the ‘List of Names’ text box, and ‘*Homo sapiens*’ was selected as the species for further analysis. The results were imported into Cytoscape software (version 3.7.0) for visualization and analysis. And the ‘Degree Value’ (the number of node-to-node interactions) and the ‘Combined Score’ were used as filtering criteria to establish the protein-protein interaction (PPI) network. The top five targets, based on the highest ‘Degree Value’, were identified as the core targets.

2.5. Gene function and pathway enrichment analysis of potential targets for PFAS induced diseases

To further investigate the toxicity mechanisms of PFAS induced ThC, KC, and TeC, the relevant analyses were conducted using Metascape. Metascape is a reputable database platform that integrates resources such as Gene Ontology (GO) and the Kyoto Encyclopedia of Genes and Genomes (KEGG) [30]. Through Gene Ontology (GO) analysis, the biological processes (BP), cellular components (CC) and molecular functions (MF) of the potential toxic mechanisms of PFAS induced disease in three cancers were investigated. The top five relevant values for each category were screened, and the core toxicity pathways were further analyzed using KEGG enrichment associated with their potential targets. The intersecting targets identified in Section 2.4 were uploaded to Metascape with the parameter ‘*Homo sapiens*’. Then, the enrichment analysis results of BP, CC, MF and KEGG signal pathways were generated. Collect and visualize results that meet the following criteria: a $P < 0.01$, a minimum count of 3, and an enrichment factor > 1.5 (enrichment factor defined as the ratio of observed counts to chance expected counts).

2.6. Molecular docking analysis of PFOA, PFOS, and PFHXS with core targets

Affinity and binding sites between three PFAS compounds (PFOA, PFOS, and PFHXS) and the core toxicity targets identified in Section 2.4 were predicted at the molecular level using molecular docking techniques. This approach enabled a detailed examination of the molecular interactions between these compounds and biological organisms. The 3D structures of three PFAS compounds (small molecule ligands) were downloaded from PubChem, and the crystal structures of potential toxicity targets (referred to as large molecule receptors) were downloaded from the RCSB PDB database. Semi-flexible docking was employed using MOE (2022.02) software to minimize the energy of the three ligands and to complement or correct the crystal structure of the receptor. This process also included protonating the receptor and pretreating it with aqueous solvents [31]. Finally, the ligand and receptor were docked for prediction. The binding energies of both are generally considered to indicate good binding activity if below -5.0 kcal/mol, and strong binding activity if below -7.0 kcal/mol [32]. The docking results with binding energies under -5.0 kcal/mol were selected and visualized.

3. Result

3.1. Toxicity assessment of PFOA, PFOS, PFHXS

The necessary information of the three components PFOA, PFOS, and PFHXS were obtained through PubChem, including their CAS numbers and SMILES numbers, as shown in Table 1. Combined with the results of ProTox 3.0, ADMETlab 2.0 and Vnn-ADMET, the LD50 values of rodents were predicted to be PFOA 518 mg/kg, PFOS 154 mg/kg and PFHXS 154 mg/kg, respectively. As shown in

Fig. 1, PFOA, PFOS, and PFHXS could potentially cause skin sensitization, corrosive irritation to the eyes, respiratory toxicity, hepatotoxicity, nephrotoxicity, and genotoxicity. This aligns with previous reports of PFAS-related toxicity. Interestingly, according to model predictions, PFOS and PFHXS might cross the blood-brain barrier. However, no studies have confirmed the function of PFAS to cross the blood-brain barrier, and further research is needed. These preliminary toxicity assessments lay groundwork for us to explore the potential toxicity mechanisms of PFAS.

3.2. Targets analysis of PFOA, PFOS, and PFHXS induce ThC, KC, and TeC

53, 45 and 52 PFOA, PFOS and PFHXS targets were screened from ChEMBL, STITCH, SwissTarget Prediction and PharmMapper databases, respectively. The network Venn diagrams and Upset Venn diagrams of these three chemicals were displayed in **Fig. 2A** and **B**. PFOA and PFOS have 22 common targets. The three chemicals share 13 common targets, and after integrating and removing duplicates, a total of 108 unique targets have been identified for PFAS.

In addition, a total of 2391 ThC targets, 3436 KC targets and 1921 TeC targets were mined and integrated from GeneCards, OMIM, Drugbank, TTD and DisGenet databases. The 108 PFAS component targets previously identified were compared with these disease-specific targets. 37 intersected targets with ThC, 45 with KC, and 30 with TeC were identified. The corresponding Venn diagrams were illustrated in **Fig. 3A, B, and C**.

3.3. PPI networks analysis

The PPI networks were constructed for the intersecting targets of PFAS and diseases using STRING and visualized them with Cytoscape, as depicted in **Fig. 3D, E, and F**. The top five targets of ThC induced by PFAS were ALB, mTOR, MDM2, ERBB2, and IL10. Similarly, for PFAS-induced KC, the top five targets included ALB, ERBB2, MDM2, IL10, and ABCB1. In TeC, the targets with the highest 'Degree value' influenced by PFAS were ALB, ERBB2, mTOR, IL10, and AR. The top five targets of PFAS induced diseases were taken as the core targets and performed an intersection analysis, as shown in **Fig. 3G**. These targets will be utilized in subsequent molecular docking analyses.

3.4. Enrichment analysis of potential toxic targets

GO analysis (including BP, CC, and MF) and KEGG pathway analysis were conducted on Metascape for the 37 targets induce by PFAS in thyroid cancer, 45 targets in renal cancer, and 30 targets in testicular cancer. The results were visualized using bar, bubble plots to illustrate the associations found in the GO enrichment analysis, as shown in **Figs. 4 and 5**. And the sankey-bubble plots were created as shown in **Fig. 6**. It was found that PFAS mainly regulated reactive oxygen species metabolism and phosphatidylinositol 3-kinase/protein kinase B signal transduction, thereby inducing the biological processes of ThC, KC and TeC. Through molecular functions such as nuclear receptor activity and kinase binding, PFAS could affect the lumen of secretory granules and the folded membranes of cells. The potential toxicity mechanisms were associated with cancer pathways, chemical carcinogenesis-reactive oxygen species/receptor activation, the FoxO signaling pathway, and neuroactive ligand-receptor interaction.

Additionally, KEGG enrichment analysis revealed some intriguing findings. The prostate cancer pathway was highly enriched in PFAS induce thyroid cancer, which has also noted in related studies [33]. This enrichment may be linked to hormonal regulatory changes. Moreover, the connection between PFAS-induced renal cancer and thyroid hormones was observed, with reports of thyroid cancer metastasizing to renal cancer [34]. These findings underscored the complexity of disease relationships but also highlighted how enrichment analysis could provide valuable insights and research directions.

3.5. Molecular docking analysis of PFOA, PFOS, PFHXS and core targets

The seven core targets induced by PFAS, ALB, mTOR, MDM2, ERBB2, IL10, ABCB1, and AR were selected as macromolecular receptors. This enabled us to explore specific interactions, such as PFOA with IL10 and ABCB1, PFOS with ALB, mTOR, and AR, and PFHXS with mTOR, MDM2 and ERBB2. It was found that the H atom of the PFOA hydroxyl group acted as a donor, forming a hydrogen bond with the O atom of the amino acid residue Glu 145 on the IL10 target. Conversely, the O atom of its carbonyl group served as an acceptor, forming a hydrogen bond with the H atom of Lys 163. Furthermore, our analysis revealed no superior docking scenarios for PFOA with ABCB1. The H atoms of the PFOS hydroxyl group function as donors, formed hydrogen bonds with the O atoms of Asp 187 and Leu 115 on the ALB target, the O atoms of Asn 2071 on the mTOR target, and the O atoms of Glu 837 and Gln 733 on the AR target. Similarly, the H atoms of the PFHXS hydroxyl group also acted as donors to form hydrogen bonds with the O atoms of Glu 2067 on the mTOR target, the O atoms of Lys 70 and Glu 69 on the MDM2 target. The O atoms of PFOS carbonyl group acted as acceptors to form

Table 1
Information about PFOA, PFOS, PFHXS.

Name	Acronyms	CAS	SMILES	LD50 (mg/kg)
Perfluorooctane sulfonic acid	PFOS	1763-23-1	<chem>C(C(C(C(C(F)F)S(=O)(=O)O)(F)F)(F)F)(C(C(C(F)F)F)(F)F)(F)F</chem>	518
perfluorocaprylic acid	PFOA	335-67-1	<chem>C(=O)C(C(C(C(C(C(F)F)(F)F)(F)F)(F)F)(F)F)O</chem>	154
Perfluorohexanesulfonic acid	PFHxS	355-46-4	<chem>C(C(C(C(F)F)S(=O)(=O)O)(F)F)(F)F(C(C(F)F)F)(F)F</chem>	154

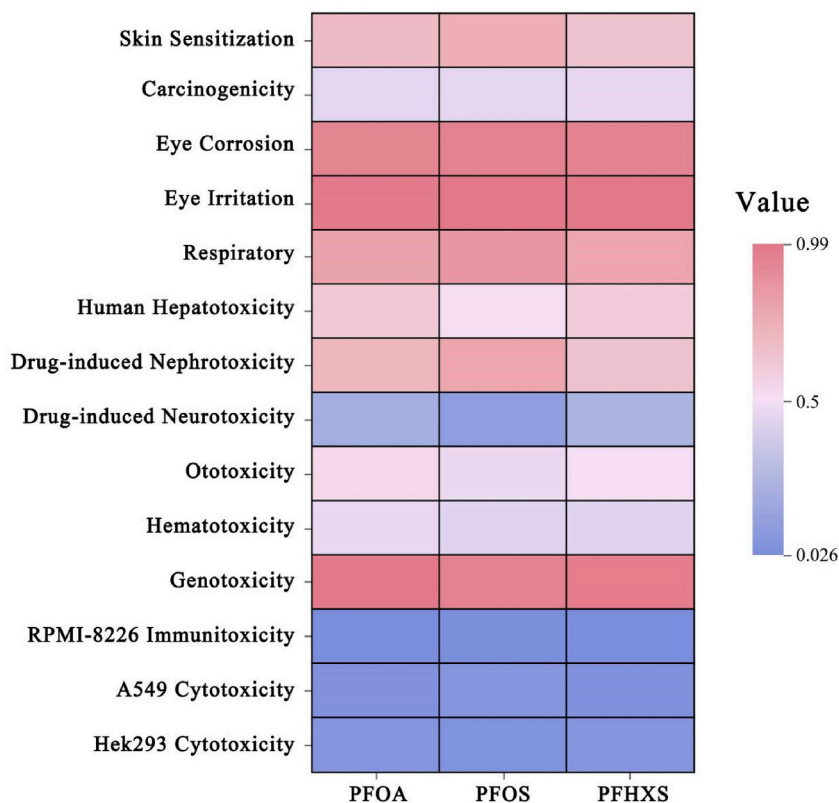


Fig. 1. Prediction of potential toxicity of PFOA, PFOS, PFHXS by modeling. The heat map vertically displayed 14 toxic phenomena that PFOA, PFOS, and PFHXS induced in the human body. Numerical bars on the right side showed the probability of each phenomenon occurring, with a high probability indicated in pink and a low probability in light purple. The closer the value was to 1, the higher the likelihood that the corresponding component caused the specified toxic phenomenon in the human body.

hydrogen bonds with the H atoms of Asp 769 and Glu 770 on the ERBB2 target. The O atom of the PFHXS carbonyl group also acted as an acceptor, forming a hydrogen bond with the H atom on MDM2 target Met 17. Small molecules occupying the same docking site exhibited different conformations and binding energies, as shown in Table 2. The docking results were visually represented through a 2D map, a 3D map, and an electrostatic energy map of the protein surface, as shown in Fig. 7 (Only the lowest binding energy site is displayed). The electrostatic energy map was created by generating the protein's molecular surface using MOE software, establishing molecular docking pockets, and visualizing the area using electrostatic properties to color the image.

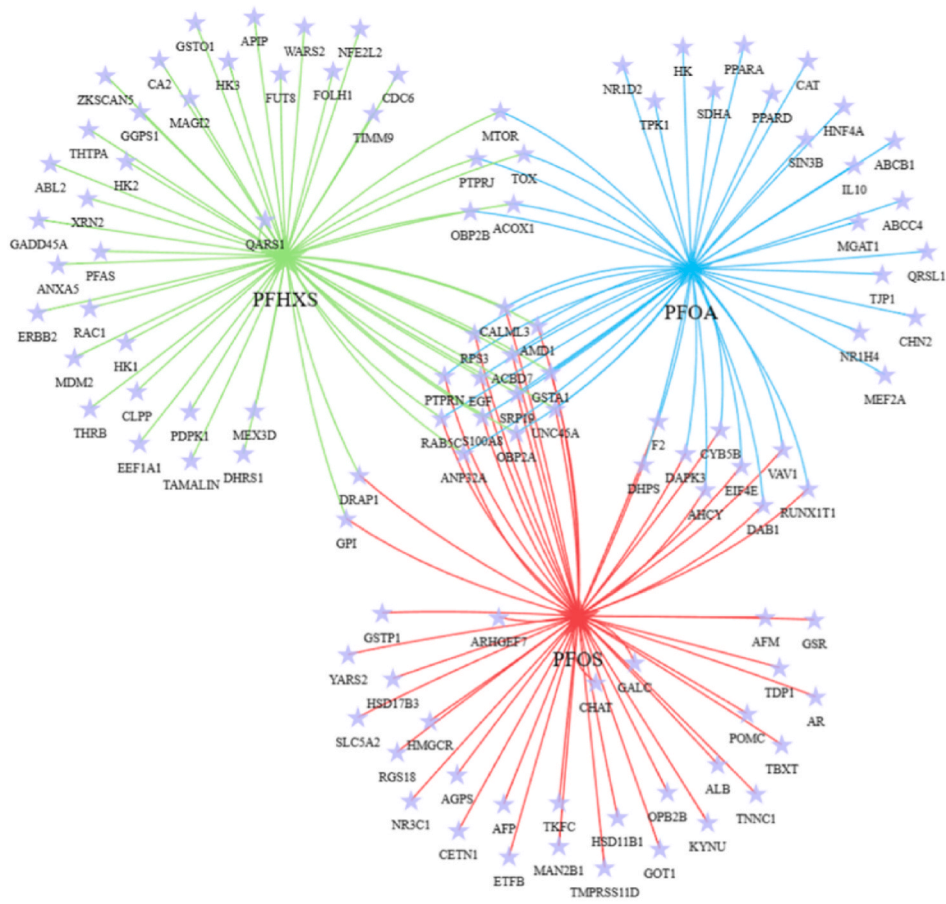
In addition, to conduct a more comprehensive analysis of the docking interactions between PFOA, PFOS, and PFHXS with the seven targets, we expanded our study to include targets that had not been previously docked molecularly. The results of these additional analyses were detailed in Supplementary Table 2 and Supplementary Figs. 1–17. These findings highlighted that ABCB1 did not demonstrate superior docking sites with either PFOS or PFHXS. The molecular docking results for these two compounds showed better binding activity, even though their constituents were not initially identified as targets in our database mining. For instance, the Upset Venn diagram in 3.2 indicated that the corresponding targets for PFOS and PFHXS did not include IL10. However, our molecular docking analysis revealed that both PFOS and PFHXS exhibited strong binding activity with IL10, with binding energies of -13.9 kcal/mol and -14.7 kcal/mol, respectively. It suggested that a single constituent may bind to multiple protein targets simultaneously, or a single protein target may accommodate multiple chemical components binding concurrently.

Combining the above analysis, PFOA, PFOS, and PFHXS exhibited low binding energies with the six core targets. The different conformations of these small molecules were well-suited to the molecular docking pockets, and the electrostatic energies around the docking bonds were low. This evidence indicated that the three PFAS components had strong binding activities with the core targets of the diseases, suggesting a potential mechanism by which PFAS induced disease toxicity at the molecular level such as ThC, KC, and TeC.

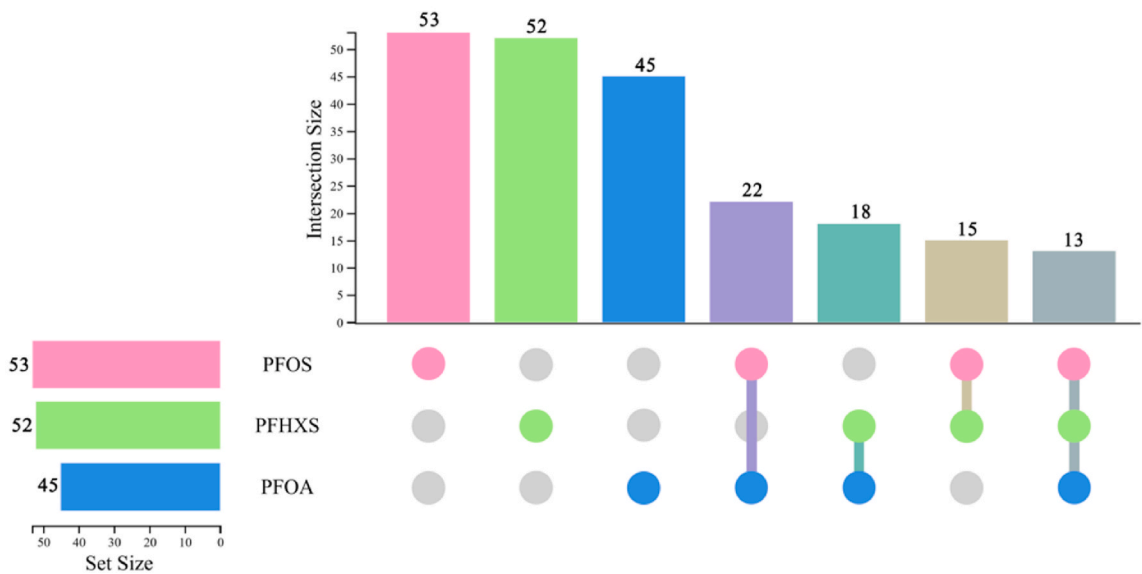
4. Discussion

Concerns about PFAS are intensifying due to its persistent environmental pollution and potential human health hazards. In response, many countries are implementing measures to restrict PFAS use and are actively seeking alternatives to mitigate its environmental and health impacts. However, many of the new alternatives to PFAS still pose threats to both the environment and human

A



B



(caption on next page)

Fig. 2. Venn diagram of PFOA, PFOS, and PFHXS enriched targets. A. The Venn diagrams illustrated the intersecting target network for PFOA, PFOS, and PFHXS. In this diagram, a purple pentagram represented each target, while the connections were color-coded: blue lines represented PFOA targets, red lines indicated PFOS targets, and green lines signified PFHXS targets. B. The Upset Venn diagram displayed the intersecting targets of PFOA, PFOS, and PFHXS. In the diagram, pink represented PFOS, green signified PFHXS, and blue denoted PFOA. The length of each bar indicated the number of targets associated with each component, while the colors of the circles below reflected the intersections among these components.

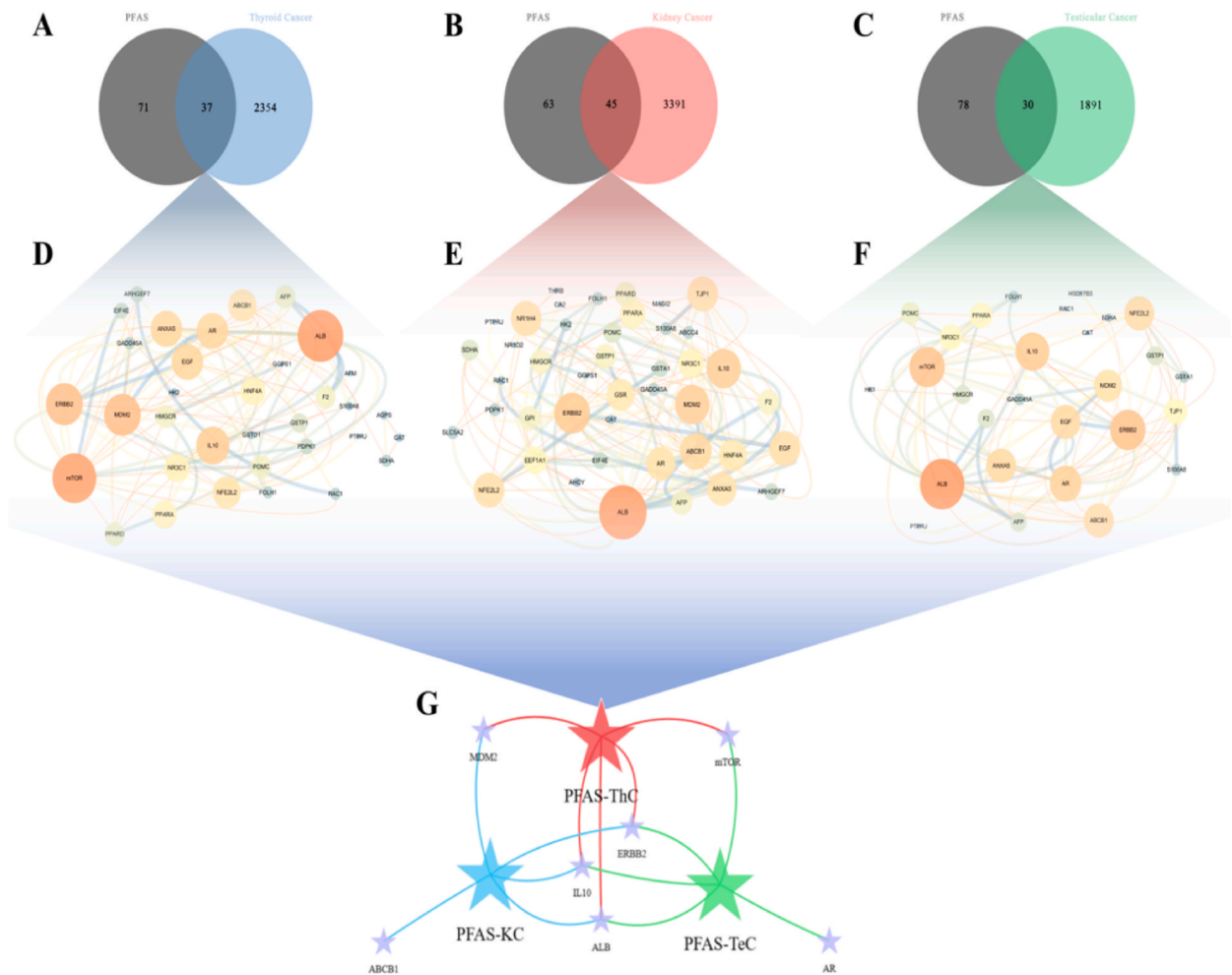


Fig. 3. Visualization of intersecting targets of PFOA, PFOS and PFHXS induced thyroid, renal and testicular cancer. A, B, and C represented the Venn diagrams of the intersecting targets of PFAS with thyroid cancer, kidney cancer, and testicular cancer, respectively. D, E, and F represented the visualize intersecting targets. Each node, represented by a circle, denoted a target, and the connecting lines between nodes depicted the interactions among these targets. Nodes with a higher 'Degree value' were shown with a larger area and a warmer color. Stronger interactions between targets were indicated by coarser connecting lines, which were colored cooler. G represented the Venn diagrams that represented the core target network of PFAS induced thyroid, kidney, and testicular cancers, indicated by red, blue, and green pentagrams, respectively. Purple pentagrams denoted the core targets.

safety [35]. At present, there is little experimental validation of the degree of cancer induction and environmental impacts of PFAS. It is likely that most environmental studies use high concentrations of PFAS for short-term exposures, which contrasts sharply with the reality that organisms are "silently" attacked over long periods by low-dose PFAS. This is akin to merely watching the trailer of a movie rather than the full feature. This short-term, high-dose experimental design does not provide a complete picture of the chain reaction and the far-reaching and complex impacts on biodiversity that may result from long-term micro-exposure to PFAS when organisms are constantly drinking from contaminated water sources and inhabiting contaminated soils. Moreover, toxicology experiments often rely on animal models, which struggle to keep pace with the rapid emergence of chemical toxins in the environment. Both in vitro and vector experiments are not only time-consuming and costly but also limited by interspecies differences. Therefore, the findings from animal experiments may not be fully applicable to humans, thereby limiting our understanding of the mechanisms of toxicity of

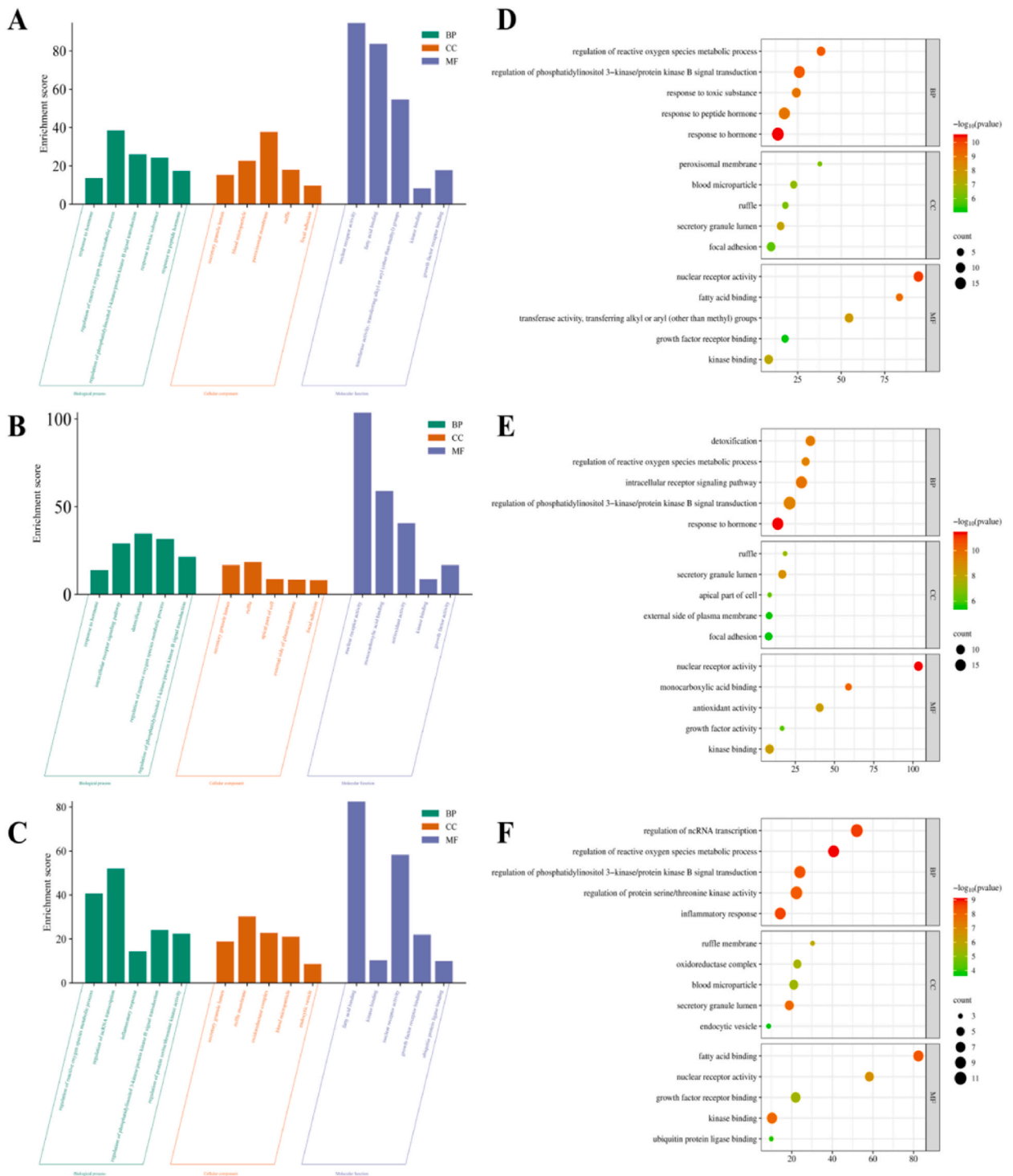
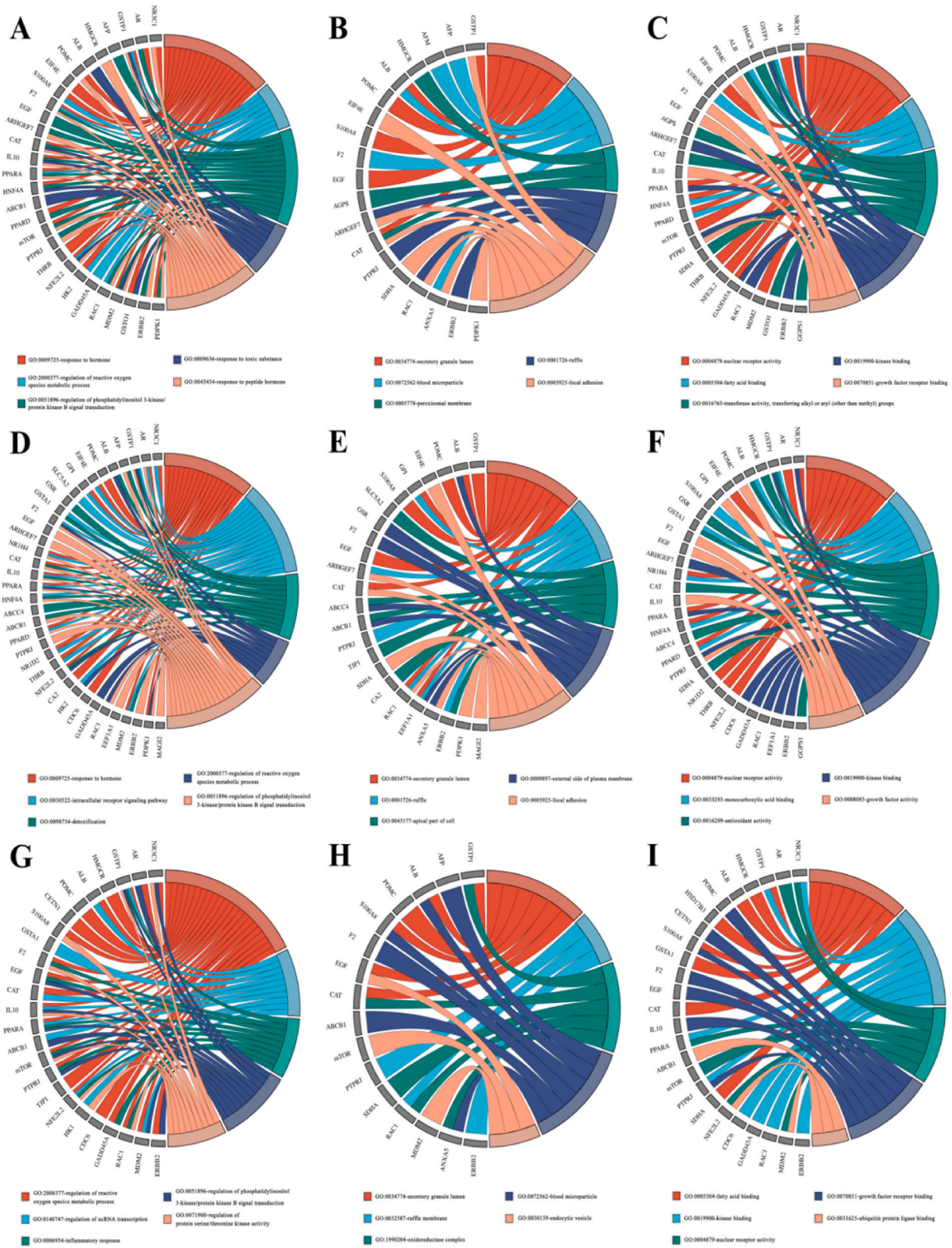


Fig. 4. GO enrichment analysis of PFAS-induced ThC, KC, TeC (top 5). A, B, and C represented the visualization of the top 5 GO enrichment analysis of PFAS induced ThC, KC, and TeC using histograms, respectively, combining BP, CC, and MF, divided by box lines, and differentiated by different colors, where the height of each square corresponded to the enrichment value, reflecting the degree of enrichment within the respective category. D, E, and F represented the visualization of the top 5 GO enrichment analysis bubble diagram of BP, CC, and MF of PFAS induced ThC, KC, and TeC. This diagram illustrated multidimensional data through the size and color of circular bubbles. The vertical axis displayed the enriched biological processes, cellular components, and molecular functions, while the horizontal axis represented the enrichment values. The size of each bubble indicated the number of targets enriched in that category, and the bubble color denoted the significance level of the enrichment, with red indicating high significance.



(caption on next page)

Fig. 5. GO enrichment analysis of PFAS-induced ThC, KC, and TeC represented by chord diagrams. A, B, and C represented chordal diagrams of BP, CC, and MF enrichment analysis of PFAS induced ThC. D, E, and F represented BP, CC, and MF enrichment analysis of PFAS induced KC. G, H, and I represented BP, CC, and MF enrichment analysis of PFAS induced TeC. These diagrams illustrated the relationships between different biological processes, cellular components, molecular functions, and their associated targets. In each diagram, the left side displayed the target, and the right side showed the enriched content. The outer circle on the left was labeled with the corresponding gene names, while the right side featured labels for different contents, each distinguished by unique colors.

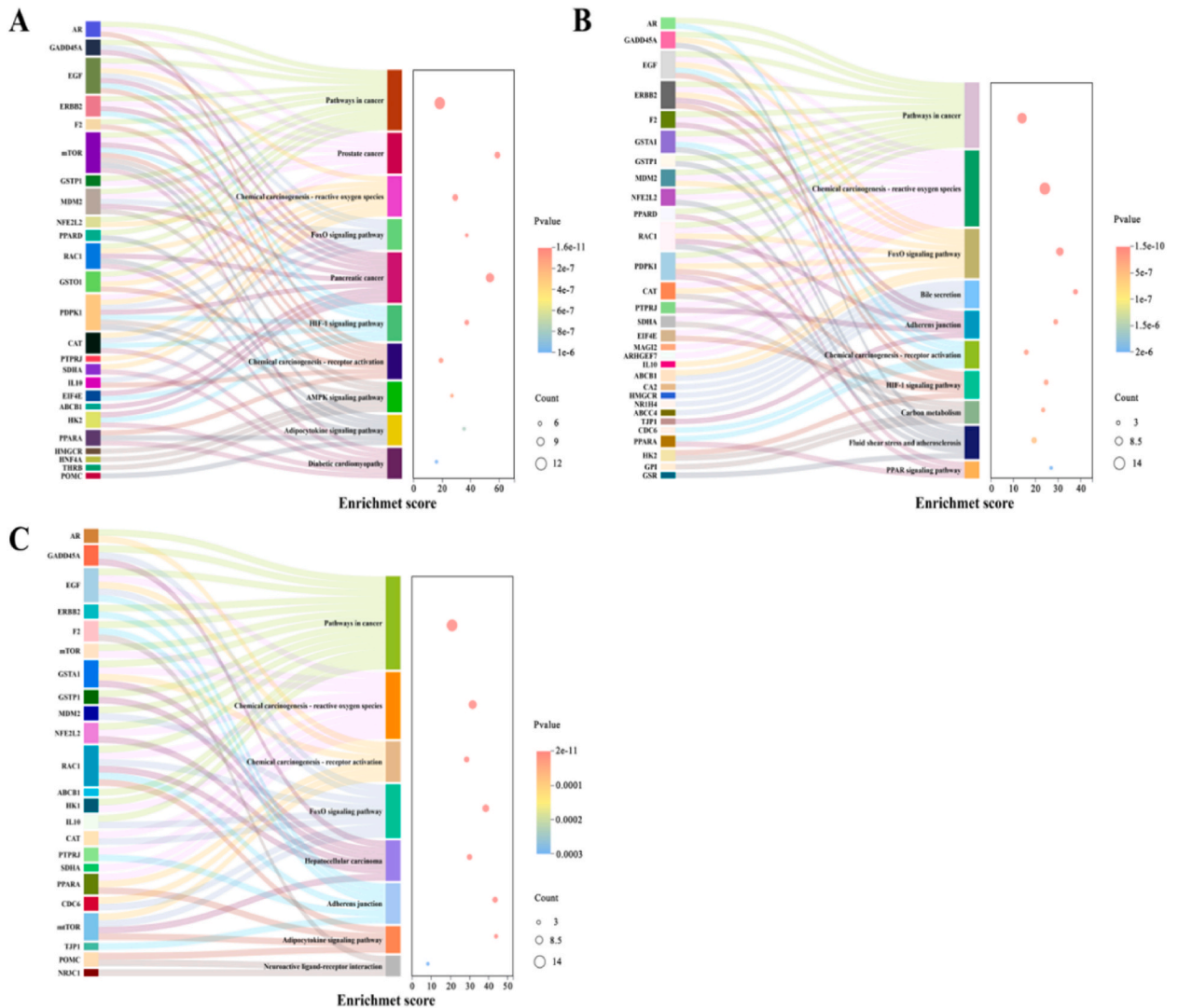
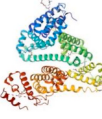

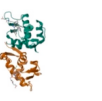

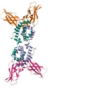



Fig. 6. The pathway enrichment analysis of PFAS-induced ThC, KC and TeC. A, B, and C presented Sankey-Bubble diagrams of pathway enrichment analysis of PFAS induced thyroid, kidney and testicular cancer, respectively. Each Sankey-Bubble diagram integrated a Sankey diagram with a bubble diagram, linked by the name of each pathway. The Sankey diagram on the left side illustrated the genes under the pathway, while the bubble diagram on the right side visualized the pathway's enrichment value through the position of the bubbles, the number of genes enriched in the pathway by the size of the bubbles, and the pathway's P-value by the color of the bubbles. Notably, a red color in the bubbles signified high significance. Among the potential pathways for PFAS-induced ThC were pathways in cancer, prostate cancer, chemical carcinogenesis-reactive oxygen species, FoxO signaling pathway, pancreatic cancer, etc. The potential pathways for PFAS-induced KC were pathways in cancer, chemical carcinogenesis-reactive oxygen species, FoxO signaling pathway, bile secretion, adherens junction, etc. The potential pathways for PFAS-induced TeC were pathways in cancer, chemical carcinogenesis-reactive oxygen species, chemical carcinogenesis-receptor activation, FoxO signaling pathway, hepatocellular carcinoma, etc.

emerging chemical substances.

Based on the above limitations in toxicology research, the importance of network toxicology and molecular docking technology is self-evident. This approach can rapidly and comprehensively map the complex molecular networks between novel toxins and

Table 2
Molecular docking information of PFOA, PFOS, PFHXS and core targets.

Target	PDB ID	Target Structure	Compound	Conformation ID	Affinity (kcal/mol)	Interaction	Receptor	Distance
ALB	6YG9		PFOS	a	-16.8	H-donor	ASP 187-O	2.73
				b	-10.1		LEU115-O	2.77
				c	-8.9			2.83
mTOR	5WBH		PFOS	a	-8.0		ASN 2071-O	2.86
				b	-7.7			2.85
				c	-7.3			2.92
			PFHXS	a	-14.1		GLU 2067-O	2.77
				b	-13.2			2.76
				c	-12.8			2.73
MDM2	5J7G		PFHXS	a	-7.4	H-donor	LYS 70-O	2.85
				b	-7.1		GLU 69-O	3.03
				c	-6.6		H-acceptor	MET 17-
ERBB2	7PCD		PFHXS	a	-10.2	H-donor	ASP 769-O	2.86
				b	-5.9		GLU 770-O	2.74
IL10	1Y6K		PFOA	a	-8.5	H-donor	GLU145-O	2.84
				b	-8.1			2.90
				c	-6.0		H-acceptor	LYS 163-H
AR	3L3X		PFOS	a	-12.2	H-donor	GLU 837-O	2.82
				b	-7.8		GLN 733-O	2.80

pathological endpoints by integrating bioinformatics, genomics, and big data technologies. It not only identifies common toxicity mechanisms but also optimizes the identification of key and core targets of toxicity phenotypes. In particular, molecular docking technology has demonstrated significant value in modeling complex structural biomolecules and molecular mechanisms. Furthermore, the use of network toxicology and molecular docking techniques not only improves the efficiency and predictive accuracy of toxicological screening but also helps to evaluate urgent environmental toxins that have not been adequately studied [36].

In this study, we integrated network toxicology and molecular docking techniques to explore the potential toxicity mechanisms of the three PFAS components, PFOA, PFOS, and PFHXS, in thyroid, kidney, and testicular cancers. The six core targets, ALB, mTOR, MDM2, ERBB2, IL10, and AR, as pivotal in the disease processes induced by PFAS. Notably, ALB, ERBB2, and IL10 emerged as common targets across PFAS induced thyroid, kidney, and testicular cancers, underscoring their critical roles in these malignancies. In addition, all three compounds, PFOA, PFOS, and PFHXS, contain long chains of perfluorocarbons (i.e., all hydrogen atoms are replaced by fluorine atoms), making them highly chemically and thermally stable. Specifically, the chemical formula of PFOA is $C_8HF_{15}O_2$, with a carboxylate group (-COOH) attached to the end, and the chemical formulas of PFOS and PFHXS are $C_8HF_{17}O_3S$ and $C_6HF_{13}O_3S$, respectively, both of which have a sulfonic acid group (-SO₃H) attached at the end. Combined with the molecular docking results, we found that the structure of all three compounds exhibits strong binding activity to the core target through the terminal hydroxyl group (-OH), which suggests that the carboxylic acid group (-COOH) in PFOA and the sulfonic acid group (-SO₃H) in PFOS and PFHXS may interact differently with biomolecules in different metabolic pathways, thus affecting their toxicity. Moreover, the polarity of the sulfonic acid group may make PFOS and PFHXS more likely to bind to proteins, which may interfere with cellular functions and lead to cellular damage and carcinogenesis.

In oncology research, ALB is primarily studied as a prognostic factor, with its levels commonly used to assess nutritional and inflammatory status. These levels indirectly influence the outcomes of oncological treatments [37]. Mutations in the IIA sub-structural domain of ALB at residue R218 are linked to familial dysalbuminemic hyperthyroxinemia (FDH) [38]. In thyroid and renal cancers, the presence of low ALB levels has been observed [39,40]. Also, a positive correlation between ALB levels and the risk of subsequent development of testicular cancer has been established in patients [41]. ERBB2/HER2, a member of the epidermal growth factor (EGF) receptor family of receptor tyrosine kinases, is closely associated with the occurrence and development of various cancers due to its aberrant expression or activation. In thyroid cancer, the expression of ERBB2 correlates with the aggressiveness of the cancer and overall prognosis. Notably, high levels of ERBB2 are found in certain subtypes of thyroid cancer, particularly in patients with metastatic thyroid cancer [42]. In kidney cancer, ERBB2 expression in normal tissues exhibits a negative correlation with its expression in renal cell carcinoma (RCC). Importantly, an increase in ERBB2 expression is observed alongside RCC tumorigenesis, indicating its potential role in the progression and development of renal cancer [43]. Studies on ERBB2 in testicular cancer are relatively limited.

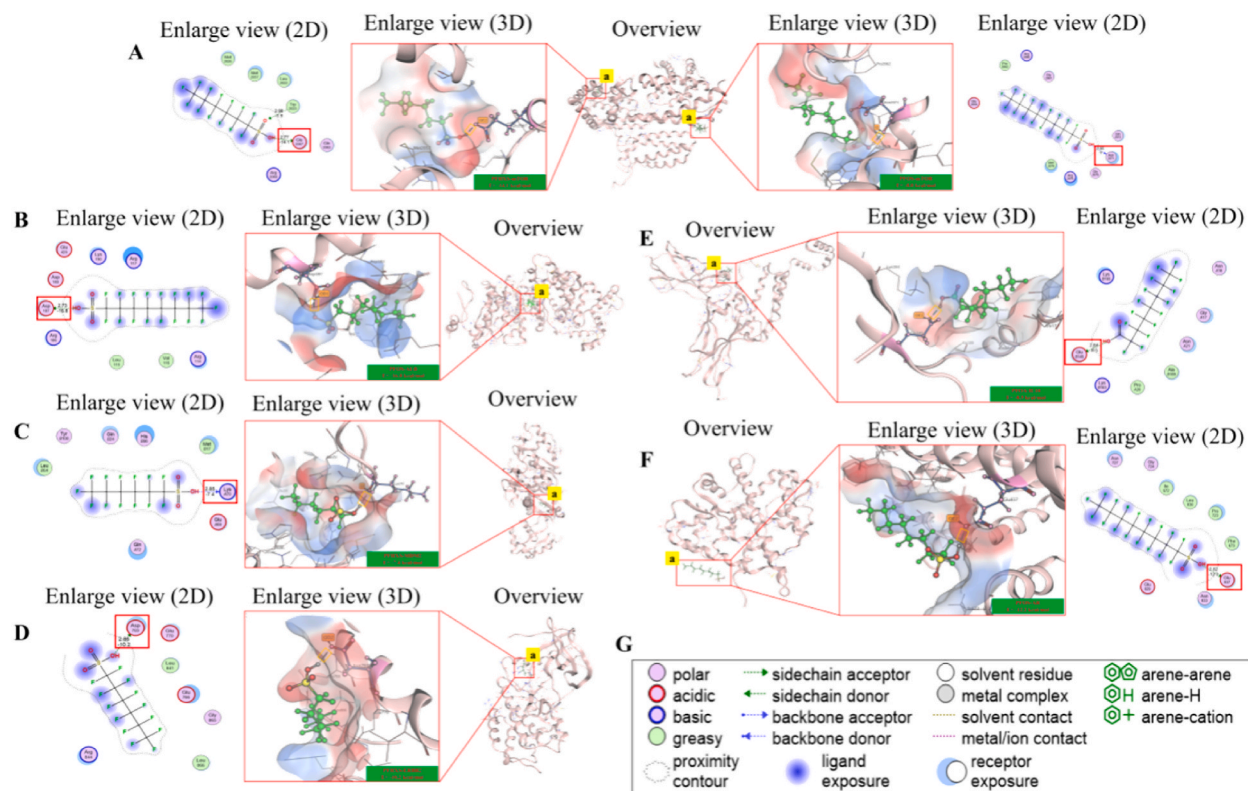


Fig. 7. Molecular docking of PFOA, PFOS, PFHXS and corresponding enriched targets. A showed the docking of PFHXS (left) and PFOS (right) with mTOR. B showed the docking of PFOS with ALB. C and D showed the docking of PFHXS with MDM2 and ERBB2, respectively. E showed the docking of PFOA and IL10. F showed the docking of PFOS with AR. G was a legend for the 2D docking diagram, including the type of binding bond and the solvent environment of amino acids. Small molecule 2D structures and amino acid docking were shown in Enlarge view (2D), and important amino acids docked to the small molecule are circled in red boxes. PFOA is docked to GLU145 of IL10; PFOS is docked to ASP187 of ALB, ASN2071 of mTOR, and GLU837 of AR, respectively; PFHXS is docked to GLU2067 of mTOR, LYS70 of MDM2, and ASP769 of ERBB2. In Enlarge view (3D) green was the small molecule ligand, blue-pink was the docked amino acid residue, both were shown in a ball-and-stick model, light pink was the large molecule receptor, the docking atoms of the residues and the binding bonds were marked with boxes, and the electrostatic energy diagram of the protein surface was shown in blue (high-energy) and red (low-energy), and the binding energies were shown in the lower right corner.

However, there is evidence suggesting that ERBB2 may play a key role in certain subtypes of testicular germ cell tumors. Crucially, it has been found that its phosphorylation is inhibited by lapatinib, a treatment that effectively blocks tumor growth [44].

IL10 is a cytokine primarily known for its role in inhibiting the activity of Th1 cells and reducing the production of pro-inflammatory cytokines, playing a crucial role in immune regulation and inflammatory responses. In the tumor microenvironment, IL-10's role is complex and dualistic. It can either promote tumor escape from immune surveillance or act as an inhibitor of tumor development depending on the specific context [45]. IL-10 is typically expressed at high levels in tumor-infiltrating lymphocytes within thyroid cancer tissues and renal cell carcinoma, potentially aiding tumor cells in evading the immune system. In the immune microenvironment, certain conditions may facilitate tumorigenesis by enabling it to avoid an effective immune response. Thus, IL-10 emerges as a potent immunosuppressive cytokine, playing a key role in tumor escape from immune surveillance. This mechanism may promote the survival and spread of thyroid cancer cells [46]. In renal cell carcinoma, a negative correlation has been identified between IL-10-producing B cells and T cell proliferation, suggesting that IL-10-producing B cells may contribute to T cell immunosuppression. This interaction indicates that B cells could play a crucial role in modulating the immune response within the tumor microenvironment, potentially facilitating tumor growth by suppressing T cell activity [47]. The role of IL-10 in testicular cancer may mirror the dynamics observed in description above, as it is secreted at high levels by testicular macrophages. These macrophages inhibit T cell proliferation and activation, and also induce immature T cells to differentiate into immunosuppressive regulatory T cells. This process promotes tumor cell escape through immunosuppressive mechanisms, enabling the cancer cells to evade immune detection and intervention effectively [48]. mTOR, a member of the phosphatidylinositol 3-kinase-associated kinase family, plays a crucial role in cancer development. Although mTOR was not enriched in kidney cancer in our study, mTOR signaling is typically activated in tumors. This includes the pivotal PI3K-AKT-mTOR pathway, which regulates cancer cell metabolism by altering the expression and activity of key metabolic enzymes. This pathway contributes significantly to tumor growth, angiogenesis, and metastasis and is particularly influential in the development of thyroid, kidney, and testicular cancers. Mutations in the mTOR gene are rare in thyroid cancer; however, there is a positive correlation between mortality and the activation of the mTOR pathway in thyroid

cancer patients with BRAF-V600E mutations [49]. Also, mTOR signaling activation is implicated in the pathogenesis of autosomal dominant polycystic kidney disease and renal cell carcinoma, where it promotes renal cyst formation and enhances RCC cell survival [50]. In testicular cancer, the PI3K/AKT/mTORC1/2 pathway is highly active in cell lines and shows a negative correlation with cisplatin induce apoptosis in testicular cancer cells [51].

MDM2, also known as E3 ubiquitin ligase, affect both thyroid and kidney cancers in our study. It induces tumor formation by targeting tumor suppressor proteins, such as p53, for proteasomal degradation. MDM2 expression is upregulated in various cancers, leading to a loss of p53-dependent activity. In a comprehensive pan-cancer analysis, MDM2 was identified as one of the genes with the highest significance for recurrent amplification across multiple cancer genomes. The analysis covered thyroid carcinoma, adrenocortical carcinoma, and testicular germ-cell tumors [52], highlighting that MDM2 not only has a strong association with thyroid and renal cancers but also plays a crucial role in the developmental course of testicular cancer. AR, an androgen receptor, functions as a steroid hormone-activated transcription factor and is typically associated with the regulation of sex hormones, reproductive function, and the development of sex-specific disorders. AR was predominantly identified in testicular cancer during our screening, aligning with relevant studies. AR has also been found to influence the development of thyroid and kidney cancers. Androgen stimulation of AR induces cellular senescence, and AR-dependent senescence effectively inhibits thyroid cancer cell growth by producing anti-inflammatory SASP factors while simultaneously reducing chemokines that promote tumor development [53]. Moreover, it has been demonstrated that elevated AR expression is positively associated with tumor angiogenesis in patients with clear cell renal cell carcinoma and significantly influences the progression of this cancer type [54].

On the other hand, the results of our enrichment analysis suggest that PFAS regulates reactive oxygen species metabolism to induce thyroid, kidney, and testicular cancers. Its potential toxicity mechanism is related to several key pathways including pathways in cancer, chemical carcinogenesis-reactive oxygen species, chemical carcinogenesis-receptor activation, FoxO signaling pathway and neuroactive ligand-receptor interactions, which may be related to targets such as ERBB2, IL-10, and MDM2. Reactive oxygen species (ROS) and cellular receptors play key roles in chemical carcinogenesis. The perfluorocarbon chains and terminal hydroxyl groups (-OH) of the three compounds, PFOA, PFOS, and PFHXS, may activate receptors on the cell surface or inside the cell, causing alterations in cellular signalling. Our molecular docking analyses have confirmed the strong binding activity of PFAS with core targets of the disease. ROS may also be involved in this process, either directly or indirectly affecting the genetic material of cells, leading to DNA damage and gene mutations, thereby promoting tumorigenesis and progression [55]. In addition, the relationship between the FoxO signaling pathway and kinase binding cannot be ignored in PFAS induce cancers. The FoxO family is involved in cellular functions such as cell differentiation, apoptosis, and cell proliferation. Dysfunction of its proteins is closely associated with cancer progression and tumorigenesis [56,57]. FoxO can act as a mediator of oxidative stress [58], establishing its significant role among tumor suppressors. Among the enrichment analysis, it is worth drawing our attention to the fact that PFAS can regulate the signaling of phosphatidylinositol 3-kinase/protein kinase B. The PI3K-AKT signaling pathway is critical in tumorigenesis, and it is one of the most frequently over-activated intracellular pathways in cancer. M-TOR also has a key role in the PI3K-AKT and FOXO signalling pathways. PFAS may activate PI3K, which transmits signals to AKT, which activates Rheb GTPase by directly phosphorylating and inhibiting the TSC1/TSC2 complex, thereby activating mTORC1, which further inhibits members of the FOXO transcription factor family (FOXO1, FOXO3A, FOXO4) regulates cell survival and proliferation. This inhibition subsequently induces cancer initiation and progression. When unactivated, FoxO is active in the nucleus and facilitates the expression of genes associated with apoptosis and metabolic homeostasis. However, once AKT is activated, it phosphorylates the FoxO transcription factor, prompting it to migrate from the nucleus to the cytoplasm. This migration effectively inhibits the transcriptional activity of FoxO, thereby reducing the rate of apoptosis and enhancing cell survival, FoxO also maintains cellular homeostasis by inhibiting mTOR signaling and initiating protective gene expression under energy-deficient and stressful conditions [59,60].

Our prediction and analysis of the potential toxicity mechanism of PFAS carcinogenesis provide a theoretical basis for the development of experiments in this field. However, validation of relevant ecotoxicity experiments and environmental exposure modeling experiments remains indispensable to ensure the accuracy of computationally based analysis results. Future studies should combine extensive epidemiological data and animal model validation to further clarify the key targets and pathways, thereby developing effective preventive and therapeutic strategies against PFAS.

5. Conclusion

The potential toxicity and mechanism of three PFAS components, PFOA, PFOS and PFHXS, were analyzed by molecular docking technology. A total of 108 targets were obtained, including 37 relevant targets for the induction of thyroid cancer, 45 relevant targets for the induction of kidney cancer, and 30 relevant targets for the induction of testicular cancer by PFOA, PFOS and PFHXS. Through enrichment analysis and molecular docking analysis, it was predicted that chronic exposure to PFAS may induce thyroid, renal, and testicular cancers by mediating six core targets: ALB, mTOR, MDM2, ERBB2, IL10, and AR. These targets regulated reactive oxygen species metabolism and phosphatidylinositol 3-kinase/protein kinase B signal transduction. Furthermore, the potential mechanisms of toxicity were closely related to various pathways, including pathways in cancer, chemical carcinogenesis-reactive oxygen species/receptor activation, the FoxO signaling pathway and neuroactive ligand-receptor interactions.

Funding sources

This research is supported by Jilin Province Science and Technology Development Project (grant number 20230204006YY).

Data availability

Data will be made available on request.

CRediT authorship contribution statement

Zhi Lin: Formal analysis, Writing – original draft. **Yvmo Li:** Data curation. **Jiarui Zhao:** Methodology. **Jun Li:** Software. **Shuang Pan:** Visualization. **Xinhe Wang:** Conceptualization. **He Lin:** Conceptualization, Writing – review & editing. **Zhe Lin:** Supervision, Writing – review & editing.

Declaration of competing interest

The authors declare that they have no known competing financial interests or personal relationships that could have appeared to influence the work reported in this paper.

Appendix. ASupplementary data

Supplementary data to this article can be found online at <https://doi.org/10.1016/j.heliyon.2024.e37003>.

References

- [1] F. Calore, P.P. Guolo, J. Wu, Q. Xu, J. Lu, A. Marcomini, Legacy and novel PFASs in wastewater, natural water, and drinking water: occurrence in Western Countries vs China, *Emerging Contam.* 9 (2023) 100228, <https://doi.org/10.1016/j.emcon.2023.100228>.
- [2] J.A. Field, J. Seow, Properties, occurrence, and fate of fluorotelomer sulfonates, *Crit. Rev. Environ. Sci. Technol.* 47 (2017) 643–691, <https://doi.org/10.1080/10643389.2017.1326276>.
- [3] R.M. Janousek, S. Lebertz, T.P. Knepper, Previously unidentified sources of perfluoroalkyl and polyfluoroalkyl substances from building materials and industrial fabrics, *Environ Sci Process Impacts* 21 (2019) 1936–1945, <https://doi.org/10.1039/c9em00091g>.
- [4] N.M. Brennan, A.T. Evans, M.K. Fritz, S.A. Peak, H.E. von Holst, Trends in the regulation of per- and polyfluoroalkyl substances (PFAS): a scoping review, *Int. J. Environ. Res. Publ. Health* 18 (2021), <https://doi.org/10.3390/ijerph182010900>.
- [5] J. Cui, P. Gao, Y. Deng, Destruction of per- and polyfluoroalkyl substances (PFAS) with advanced reduction processes (ARPs): a critical review, *Environ. Sci. Technol.* 54 (2020) 3752–3766, <https://doi.org/10.1021/acs.est.9b05565>.
- [6] C.H. Yu, C.D. Riker, S-e Lu, Z. Fan, Biomonitoring of emerging contaminants, perfluoroalkyl and polyfluoroalkyl substances (PFAS), in New Jersey adults in 2016–2018, *Int. J. Hyg Environ. Health* 223 (2020) 34–44, <https://doi.org/10.1016/j.ijheh.2019.10.008>.
- [7] H. Li, A.L. Junker, J. Wen, L. Ahrens, M. Sillanpää, J. Tian, et al., A recent overview of per- and polyfluoroalkyl substances (PFAS) removal by functional framework materials, *Chem. Eng. J.* 452 (2023) 139202, <https://doi.org/10.1016/j.cej.2022.139202>.
- [8] Y. Chen, L. Wei, W. Luo, N. Jiang, Y. Shi, P. Zhao, et al., Occurrence, spatial distribution, and sources of PFASs in the water and sediment from lakes in the Tibetan Plateau, *J. Hazard Mater.* 443 (2023) 130170, <https://doi.org/10.1016/j.jhazmat.2022.130170>.
- [9] R. Riaz, M. Junaid, M.Y.A. Rehman, T. Iqbal, J.A. Khan, Y. Dong, et al., Spatial distribution, compositional profile, sources, ecological and human health risks of legacy and emerging per- and polyfluoroalkyl substances (PFASs) in freshwater reservoirs of Punjab, Pakistan, *Sci. Total Environ.* 856 (2023) 159144, <https://doi.org/10.1016/j.scitotenv.2022.159144>.
- [10] B. Xu, W. Qiu, J. Du, Z. Wan, J.L. Zhou, H. Chen, et al., Translocation, bioaccumulation, and distribution of perfluoroalkyl and polyfluoroalkyl substances (PFASs) in plants, *iScience* 25 (2022) 104061, <https://doi.org/10.1186/s12902-023-01332-3>.
- [11] E. Panieri, K. Baralic, D. Djukic-Cosic, A. Buha Djordjevic, L. Saso, PFAS molecules: a major concern for the human health and the environment, *Toxics* 10 (2022), <https://doi.org/10.3390/toxics10020044>.
- [12] L. Schultes, R. Vestergren, K. Volkova, E. Westberg, T. Jacobson, J.P. Benskin, Per- and polyfluoroalkyl substances and fluorine mass balance in cosmetic products from the Swedish market: implications for environmental emissions and human exposure, *Environ. Sci. J. Integr. Environ. Res.: Process. Impacts* 20 (2018) 1680–1690, <https://hub.uu2025.xyz/10.1039/c8em00368h>.
- [13] M. Zarębska, S. Bajkacz, Z. Hordyjewicz-Baran, Assessment of legacy and emerging PFAS in the Oder River: occurrence, distribution, and sources, *Environ. Res.* 251 (2024) 118608, <https://doi.org/10.1016/j.envres.2024.118608>.
- [14] R. Ghisi, T. Vamerali, S. Manzetti, Accumulation of perfluorinated alkyl substances (PFAS) in agricultural plants: a review, *Environ. Res.* 169 (2019) 326–341, <https://doi.org/10.1016/j.envres.2018.10.023>.
- [15] R. Vestergren, I.T. Cousins, 12 - human dietary exposure to per- and poly-fluoroalkyl substances (PFASs), in: M. Rose, A. Fernandes (Eds.), *Persistent Organic Pollutants and Toxic Metals in Foods*, Woodhead Publishing, 2013, pp. 279–307, <https://doi.org/10.1533/9780857098917.2.279>.
- [16] E.M. Sunderland, X.C. Hu, C. Dassuncao, A.K. Tokranov, C.C. Wagner, J.G. Allen, A review of the pathways of human exposure to poly- and perfluoroalkyl substances (PFASs) and present understanding of health effects, *J. Expo. Sci. Environ. Epidemiol.* 29 (2019) 131–147, <https://doi.org/10.1038/s41370-018-0094-1>.
- [17] W. Hu, M.Y. Zhang, L.Y. Liu, Z.F. Zhang, Y. Guo, Perfluoroalkyl and polyfluoroalkyl substances (PFASs) crossing the blood-cerebrospinal fluid barrier: their occurrence in human cerebrospinal fluid, *J. Hazard Mater.* 442 (2023) 130003, <https://doi.org/10.1016/j.jhazmat.2022.130003>.
- [18] Y. Liu, X. Zhou, Y. Wu, X. Yang, Y. Wang, S. Li, et al., Exposure and blood–cerebrospinal fluid barrier permeability of PFASs in neonates, *Environ. Sci. Technol. Lett.* 9 (2022) 64–70, <https://doi.org/10.1021/acs.estlett.1c00862>.
- [19] J.M. Jian, D. Chen, F.J. Han, Y. Guo, L. Zeng, X. Lu, et al., A short review on human exposure to and tissue distribution of per- and polyfluoroalkyl substances (PFASs), *Sci. Total Environ.* 636 (2018) 1058–1069, <https://doi.org/10.1016/j.scitotenv.2018.04.380>.
- [20] J.J. Liu, X.X. Cui, Y.W. Tan, P.X. Dong, Y.Q. Ou, Q.Q. Li, et al., Per- and polyfluoroalkyl substances alternatives, mixtures and liver function in adults: a community-based population study in China, *Environ. Int.* 163 (2022) 107179, <https://doi.org/10.1016/j.envint.2022.107179>.
- [21] M. Averina, J. Brox, S. Huber, A.S. Furberg, Exposure to perfluoroalkyl substances (PFAS) and dyslipidemia, hypertension and obesity in adolescents. The Fit Futures study, *Environ. Res.* 195 (2021) 110740, <https://doi.org/10.1016/j.envres.2021.110740>.
- [22] X. Feng, G. Long, G. Zeng, Q. Zhang, B. Song, K.H. Wu, Association of increased risk of cardiovascular diseases with higher levels of perfluoroalkylated substances in the serum of adults, *Environ. Sci. Pollut. Res. Int.* 29 (2022) 89081–89092, <https://doi.org/10.1007/s11356-022-22021-z>.
- [23] M. van Gerwen, E. Colicino, H. Guan, G. Dolios, G.N. Nadkarni, R.C.H. Vermeulen, et al., Per- and polyfluoroalkyl substances (PFAS) exposure and thyroid cancer risk, *EBioMedicine* 97 (2023) 104831, <https://doi.org/10.1016/j.ebiom.2023.104831>.

- [24] Z. Sun, Y. Wen, B. Wang, S. Deng, F. Zhang, Z. Fu, et al., Toxic effects of per- and polyfluoroalkyl substances on sperm: epidemiological and experimental evidence, *Front. Endocrinol.* 14 (2023) 1114463, <https://doi.org/10.3389/fendo.2023.1114463>.
- [25] K. Luo, W. Huang, Q. Zhang, X. Liu, M. Nian, M. Wei, et al., Environmental exposure to legacy poly/perfluoroalkyl substances, emerging alternatives and isomers and semen quality in men: a mixture analysis, *Sci. Total Environ.* 833 (2022) 155158, <https://doi.org/10.1016/j.scitotenv.2022.155158>.
- [26] S. Huang, A novel strategy for the study on molecular mechanism of prostate injury induce by 4,4'-sulfonyldiphenol based on network toxicology analysis, *J. Appl. Toxicol.* 44 (2024) 28–40, <https://doi.org/10.1002/jat.4506>.
- [27] M.M. Nowotka, A. Gaulton, D. Mendez, A.P. Bento, A. Hersey, A. Leach, Using ChEMBL web services for building applications and data processing workflows relevant to drug discovery, *Expert Opin. Drug Discov.* 12 (2017) 757–767, <https://doi.org/10.1080/17460441.2017.1339032>.
- [28] A. Daina, O. Michielin, V. Zoete, SwissTargetPrediction: updated data and new features for efficient prediction of protein targets of small molecules, *Nucleic Acids Res.* 47 (2019) W357–w364, <https://doi.org/10.1093/nar/gkz382>.
- [29] C. UniProt, UniProt: the universal protein knowledgebase in 2023, *Nucleic Acids Res.* 51 (2023) D523–D531, <https://doi.org/10.1093/nar/gkac1052>.
- [30] Y. Zhou, B. Zhou, L. Pache, M. Chang, A.H. Khodabakhshi, O. Tanaseichuk, et al., Metascape provides a biologist-oriented resource for the analysis of systems-level datasets, *Nat. Commun.* 10 (2019) 1523, <https://doi.org/10.1038/s41467-019-09234-6>.
- [31] S.I. Alzarea, S. Qasim, M. Afzal, O.A. Alsaïdan, H.H. Alhassan, M. Alharbi, et al., Anandamide reuptake inhibitor (VDM11) as a possible candidate for COVID-19 associated depression; a combination of network pharmacology, molecular docking and in vivo experimental analysis, *Processes* 11 (2023) 143, <https://doi.org/10.3390/pr11010143>.
- [32] K.Y. Hsin, S. Ghosh, H. Kitano, Combining machine learning systems and multiple docking simulation packages to improve docking prediction reliability for network pharmacology, *PLoS One* 8 (2013) e83922, <https://doi.org/10.1371/journal.pone.0083922>.
- [33] A.S. Ho, T.J. Daskivich, W.L. Sacks, Z.S. Zumsteg, Parallels between low-risk prostate cancer and thyroid cancer: a review, *JAMA Oncol.* 5 (2019) 556–564, <https://doi.org/10.1001/jamaoncol.2018.5321>.
- [34] R. Xie, D. Tan, B. Liu, X. Han, X. Jin, D. Shen, et al., Kidney cancer with thyroid metastasis combined with thyroid carcinoma, a case report, *BMC Endocr. Disord.* 23 (2023) 95, <https://doi.org/10.1186/s12902-023-01332-3>.
- [35] N. Hamid, M. Junaid, M. Sultan, S.T. Yoganandham, O.M. Chuan, The untold story of PFAS alternatives: insights into the occurrence, ecotoxicological impacts, and removal strategies in the aquatic environment, *Water Res.* 250 (2024) 121044, <https://doi.org/10.1016/j.watres.2023.121044>.
- [36] S. Huang, Efficient analysis of toxicity and mechanisms of environmental pollutants with network toxicology and molecular docking strategy: acetyl tributyl citrate as an example, *Sci. Total Environ.* 905 (2023) 167904, <https://doi.org/10.1016/j.scitotenv.2023.167904>.
- [37] Q. Tang, X. Li, C.R. Sun, Predictive value of serum albumin levels on cancer survival: a prospective cohort study, *Front. Oncol.* 14 (2024) 1323192, <https://doi.org/10.3389/fonc.2024.1323192>.
- [38] Y. Zhang, F. Garofano, X. Wu, M. Schmid, P. Krawitz, M. Essler, et al., Integrative analysis of key candidate genes and signaling pathways in autoimmune thyroid dysfunction related to anti-CTLA-4 therapy by bioinformatics, *Invest. N. Drugs* 38 (2020) 1717–1729, <https://doi.org/10.1007/s10637-020-00952-z>.
- [39] H. Ataş, B. Korukluoğlu, B.A. Özdemir, N. Yakşi, B. Saylam, M. Tez, Diagnostic value of modified systemic inflammation score for prediction of malignancy in patients with indeterminate thyroid nodules, *Am. J. Surg.* 221 (2021) 117–121, <https://doi.org/10.1016/j.amjsurg.2020.08.002>.
- [40] H. Mao, F. Yang, Prognostic significance of albumin-to-globulin ratio in patients with renal cell carcinoma: a meta-analysis, *Front. Oncol.* 13 (2023) 1210451, <https://doi.org/10.3389/fonc.2023.1210451>.
- [41] A. Ghoshal, H. Garmo, R. Arthur, N. Hammar, I. Jungner, H. Malmström, et al., Serum biomarkers to predict risk of testicular and penile cancer in AMORIS, *Ecancermedicalscience* 11 (2017) 762, <https://doi.org/10.3332/ecancer.2017.762>.
- [42] Y. Jin, X. Qiu, Z. He, J. Wang, R. Sa, L. Chen, ERBB2 as a prognostic biomarker correlates with immune infiltrates in papillary thyroid cancer, *Front. Genet.* 13 (2022) 966365, <https://doi.org/10.3389/fgene.2022.966365>.
- [43] H. Wang, C. Liu, J. Han, L. Zhen, T. Zhang, X. He, et al., HER2 expression in renal cell carcinoma is rare and negatively correlated with that in normal renal tissue, *Oncol. Lett.* 4 (2012) 194–198, <https://doi.org/10.3892/ol.2012.727>.
- [44] M. Juliachs, W. Castillo-Ávila, A. Vidal, J.M. Piulats, X. Garcia Del Muro, E. Condom, et al., ErbBs inhibition by lapatinib blocks tumor growth in an orthotopic model of human testicular germ cell tumor, *Int. J. Cancer* 133 (2013) 235–246, <https://doi.org/10.1002/ijc.28009>.
- [45] V. Carlini, D.M. Noonan, E. Abdalalem, D. Goletti, C. Sansone, L. Calabrone, et al., The multifaceted nature of IL-10: regulation, role in immunological homeostasis and its relevance to cancer, COVID-19 and post-COVID conditions, *Front. Immunol.* 14 (2023) 1161067, <https://doi.org/10.3389/fimmu.2023.1161067>.
- [46] L.L. Cunha, E.C. Morari, S. Nonogaki, M.A. Marcello, F.A. Soares, J. Vassallo, et al., Interleukin 10 expression is related to aggressiveness and poor prognosis of patients with thyroid cancer, *Cancer Immunol. Immunother.* 66 (2017) 141–148, <https://doi.org/10.1007/s00262-016-1924-4>.
- [47] Y. Jian, K. Yang, X. Sun, J. Zhao, K. Huang, A. Aldanakh, et al., Current advance of immune evasion mechanisms and emerging immunotherapies in renal cell carcinoma, *Front. Immunol.* 12 (2021) 639636, <https://doi.org/10.3389/fimmu.2021.639636>.
- [48] S. Bhushan, M.S. Theas, V.A. Guazzone, P. Jacobo, M. Wang, M. Fijak, et al., Immune cell subtypes and their function in the testis, *Front. Immunol.* 11 (2020) 583304, <https://doi.org/10.3389/fimmu.2020.583304>.
- [49] A. Derwich, M. Sykutera, B. Bromińska, M. Andrusiewicz, M. Ruchała, N. Sawicka-Gutaj, Clinical implications of mTOR expression in papillary thyroid cancer-A systematic review, *Cancers* 15 (2023), <https://doi.org/10.3390/cancers15061665>.
- [50] Y. Gui, C. Dai, mTOR signaling in kidney diseases, *Kidney Int.* 139 (2020) 1319–1327, <https://doi.org/10.1016/j.kid.2020.03.003>.
- [51] X. Rosas-Plaza, G. de Vries, G.J. Meersma, A.J.H. Suurmeijer, J.A. Gietema, M. van Vugt, et al., Dual mTORC1/2 inhibition sensitizes testicular cancer models to cisplatin treatment, *Mol. Cancer Therapeut.* 19 (2020) 590–601, <https://doi.org/10.1158/1535-7163.MCT-19-0449>.
- [52] J.D. Oliner, A.Y. Saiki, S. Caenepel, The role of MDM2 amplification and overexpression in tumorigenesis, *Cold Spring Harb Perspect Med* 6 (2016), <https://doi.org/10.1101/cshperspect.a026336>.
- [53] A. Gupta, M. Carnazza, M. Jones, Z. Darzynkiewicz, D. Halicka, T. O'Connell, et al., Androgen receptor activation induces senescence in thyroid cancer cells, *Cancers* 15 (2023), <https://doi.org/10.3390/cancers15082198>.
- [54] B. You, Y. Sun, J. Luo, K. Wang, Q. Liu, R. Fang, et al., Androgen receptor promotes renal cell carcinoma (RCC) vasculogenic mimicry (VM) via altering TWIST1 nonsense-mediated decay through lncRNA-TANAR, *Oncogene* 40 (2021) 1674–1689, <https://doi.org/10.1038/s41388-020-01616-1>.
- [55] V. Aggarwal, H.S. Tuli, A. Varol, F. Thakral, M.B. Yerer, K. Sak, et al., Role of reactive oxygen species in cancer progression: molecular mechanisms and recent advancements, *Biomolecules* 9 (2019), <https://doi.org/10.3390/biom9110735>.
- [56] M. Farhan, H. Wang, U. Gaur, P.J. Little, J. Xu, W. Zheng, FOXO signaling pathways as therapeutic targets in cancer, *Int. J. Biol. Sci.* 13 (2017) 815–827, <https://doi.org/10.7150/ijbs.20052>.
- [57] K.K. Ho, S.S. Myatt, E.W. Lam, Many forks in the path: cycling with FoxO, *Oncogene* 27 (2008) 2300–2311, <https://doi.org/10.1038/onc.2008.23>.
- [58] B. Vurusaner, G. Poli, H. Basaga, Tumor suppressor genes and ROS: complex networks of interactions, *Free Radic. Biol. Med.* 52 (2012) 7–18, <https://doi.org/10.1016/j.freeradbiomed.2011.09.035>.
- [59] M. Hornsveid, T.B. Dansen, P.W. Derksen, B.M.T. Burgering, Re-evaluating the role of FOXOs in cancer, *Semin. Cancer Biol.* 50 (2018) 90–100, <https://doi.org/10.1016/j.semcancer.2017.11.017>.
- [60] F. Rascio, F. Spadaccino, M.T. Rocchetti, G. Castellano, G. Stallone, G.S. Netti, et al., The pathogenic role of PI3K/AKT pathway in cancer onset and drug resistance: an updated review, *Cancers* 13 (2021), <https://doi.org/10.3390/cancers13163949>.